Enhanced G1 arrest and apoptosis via MDM4/MDM2 double knockdown and MEK inhibition in wild-type *TP53* colon and gastric cancer cells with aberrant KRAS signaling

XIAOXUAN WANG[1], YOSHIYUKI YAMAMOTO[1], MAMIKO IMANISHI[1], XIAOCHEN ZHANG[1], MASASHI SATO[1], AKINORI SUGAYA[2], MITSUAKI HIROSE[1,3], SHINJI ENDO[1,4], YUKIKAZU NATORI[5], TOSHIKAZU MORIWAKI[1], KENJI YAMATO[1] and ICHINOSUKE HYODO[1,6]

[1]Department of Gastroenterology, Institute of Clinical Medicine, Graduate School of Comprehensive Human Sciences, University of Tsukuba, Tsukuba, Ibaraki 305-8575; [2]Division of Gastroenterology, Ibaraki Prefectural Central Hospital, Kasama, Ibaraki 309-1793; [3]Department of Gastroenterology, Tsuchiura Clinical Education and Training Center, University of Tsukuba Hospital, Tsuchiura, Ibaraki 300-8585; [4]Department of Gastroenterology and Hepatology, Shinmatsudo Central General Hospital, Matsudo, Chiba 270-0034; [5]BioThinkTank Co. Ltd., Yokohama, Kanagawa 220-0012; [6]Department of Gastrointestinal Medical Oncology, NHO Shikoku Cancer Center, Matsuyama, Ehime 791-0280, Japan

Received December 20, 2020; Accepted March 17, 2021

DOI: 10.3892/ol.2021.12819

Abstract. Murine double minute homolog 2 (MDM2) is an oncoprotein that induces p53 degradation via ubiquitin-ligase activity. MDM4 cooperates with MDM2-mediated p53 degradation, directly inhibiting p53 transcription by binding to its transactivation domain. Our previous study reported that the simultaneous inhibition of MDM2 and MDM4 using nutlin-3 (an inhibitor of the MDM2-p53 interaction) and chimeric small interfering RNA with DNA-substituted seed arms (named chiMDM2 and chiMDM4) more potently activated p53 than the MDM2 or MDM4 inhibitor alone and synergistically augmented antitumor effects in various types of cancer cells with the wild-type (wt) *TP53*. Recently, the synergism of MDM2 and mitogen-activated protein kinase kinase (MEK) inhibitors has been demonstrated in wt *TP53* colorectal and non-small cell lung cancer cells harboring mutant-type (mt) *KRAS*. The current study examined whether chiMDM4 augmented the synergistic antitumor effects of MDM2 and MEK inhibition using chiMDM2 or nutlin-3 and trametinib, respectively. ChiMDM2 and trametinib used in combination demonstrated a synergistic antitumor activity in HCT116 and LoVo colon cancer cells, and SNU-1 gastric cancer cells harboring wt *TP53* and mt *KRAS*. Furthermore, chiMDM4 synergistically enhanced this combinational effect. Similar results were observed when nutlin-3 was used instead of chiMDM2. MDM4/MDM2 double knockdown combined with trametinib treatment enhanced G1 arrest and apoptosis induction. This was associated with the accumulation of p53, suppression of phosphorylated-extracellular signal-regulated kinase 2, inhibition of retinoblastoma phosphorylation, suppression of E2F1-activated proteins, and potent activation of pro-apoptotic proteins, such as Fas and p53 upregulated modulator of apoptosis. The results inidcated that the triple inhibition of MDM4, MDM2 and MEK exerted a potent anti-tumor effect in wt *TP53* colon and gastric cancer cells with mt *KRAS*. Simultaneous activation of p53 and inhibition of aberrant KRAS signaling may be a rational treatment strategy for gastrointestinal tumors.

Correspondence to: Dr Yoshiyuki Yamamoto, Department of Gastroenterology, Institute of Clinical Medicine, Graduate School of Comprehensive Human Sciences, University of Tsukuba, 1-1-1 Tennodai, Tsukuba, Ibaraki 305-8575, Japan
E-mail: y-yamamoto@md.tsukuba.ac.jp

Abbreviations: chiCont, control chimeric siRNA; chiMDM2, chimeric siRNA with DNA-substituted seed arms targeting *MDM2*; chiMDM4, chimeric siRNA with DNA-substituted seed arms targeting *MDM4*; CI, combination index; wt, wild-type; mt, mutant-type

Key words: colon cancer, gastric cancer, KRAS, TP53, mitogen-activated protein kinase kinase, murine double minute homolog 2, murine double minute homolog 4, trametinib

Introduction

The tumor protein (*TP*) *53*, a tumor suppressor gene, has been reported to be inactivated mainly by missense mutation in approximately 50% of various advanced human cancers (1,2). Even in cancers carrying wild-type (wt) *TP53*, p53 is often suppressed by upregulated murine double minute homolog 2 (MDM2) and MDM4 (3). MDM2 inhibits the p53 transcriptional activity and ubiquitinates p53 leading to its degradation (4). MDM4 forms a complex with MDM2 that participates in p53 degradation. Furthermore, MDM4 can block p53-mediated transcription through direct binding to the transactivation domain of p53. MDM4 is also a target of MDM2-mediated ubiquitination and subsequent degradation (5,6). In normal

cells, an autoregulatory feedback loop formed with MDM2, MDM4, and p53 ensures a dynamic equilibrium between these molecules (4,7). In cancer cells, the regulatory relationship between these three proteins is disrupted by *TP53* mutations or *MDM2* and *MDM4* overexpression, contributing to carcinogenesis and tumor progression.

It has been expected that synthetic small interfering RNAs (siRNAs) are promising therapeutics to be applied to cancer therapy. They can be designed to specifically target cancer-driver genes in a sequence-specific manner, enabling more precise and personalized treatments (8). We previously reported that the MDM2 inhibitor nutlin-3 or siRNAs with DNA-substituted seed arms targeting *MDM2* (chiMDM2) inhibited tumor cell growth and viability by inducing G1 arrest and apoptosis in colon and gastric cancer cells carrying wt *TP53* (9-11). Furthermore, we revealed that MDM4 knockdown using chiMDM4 could greatly enhance the antitumor effects of nutlin-3 and chiMDM2 in those cancer cells via augmented p53 activation (9,10).

The interaction between the p53 pathway and the RAS-RAF-mitogen-activated protein kinase kinase (MEK)-extracellular signal-regulated kinase (ERK) cascade has been previously reported (12,13). ERK1/2 upregulates phosphorylation of MDM2 at Ser-166 and promotes MDM2-mediated p53 degradation. Dual targeting of the p53 pathway and the RAS-RAF-MEK-ERK cascade may be a rational therapeutic strategy for wt *TP53* expressing colorectal and gastric cancers with activated epidermal growth factor receptor pathways. Further, this strategy might be particularly important for tumors carrying mutant-type (mt) *RAS* and *RAF*, exhibiting resistance to antibodies targeted against these receptors. Recently, the synergism of MDM2 and MEK inhibitors was demonstrated in colorectal and non-small cell lung cancer cells harboring mt *KRAS* (14). However, the precise mechanism of action remains unclear.

In this study, we aimed to analyze whether MDM4 knockdown using chiMDM4 synergistically augments the antitumor effect of the combination of MDM2 knockdown using chiMDM2 and trametinib, a MEK1/2 inhibitor, or that of nutlin-3 and trametinib. In addition, we investigated the molecular mechanism of the antitumor effects induced by MDM4/MDM2 dual knockdown and trametinib treatment in colon and gastric cancer cells with wt *TP53* and mt *KRAS*.

Materials and methods

Cell culture. HCT116 colon cancer cell line was purchased from Horizon Discovery (Cambridge, UK). LoVo colon and SNU-1 gastric cancer cell lines were purchased from the American Type Culture Collection. HCT116 and SNU-1 cell lines were cultured in the RPMI-1640 medium (Sigma-Aldrich; Merck KGaA) supplemented with 10% heat-inactivated fetal bovine serum (FBS) (Sigma-Aldrich; Merck KGaA). LoVo cell line was cultured in Ham's F-12 nutrient mixture medium (Sigma-Aldrich; Merck KGaA) containing 10% FBS. Trametinib was purchased from Cayman Chemical (Ann Arbor). Nutlin-3 was purchased from Calbiochem.

siRNAs and transfection. Control siRNA and MDM2- and MDM4-targeting DNA-modified siRNA sequences used in this study were adopted from a previous report (10). Reverse siRNA transfection was performed using lipofectamine RNAiMAX (Invitrogen; Thermo Fisher Scientific, Inc.), in accordance with the manufacturer's instructions. Transfection of the SNU-1 cell line was performed as described previously (9). Transfection effects of chiMDM2 and chiMDM4 are shown in Fig. S1.

Cell viability and combination index. Cell viability was determined using the WST-8 colorimetric assay with the Cell Count Reagent SF (Nacalai Tesque) as previously described (9). The combination index (CI) was determined by the Chou-Talalay method using the CalcuSyn software (Biosoft) (15). The CI values of <0.9, ≥ 0.9 and <1.1, and ≥ 1.1 were defined as the synergistic effect, additive effect, and antagonistic effect, respectively.

Immunoblot analysis and cell cycle assay. Protein extraction, sodium dodecyl sulfate polyacrylamide gel electrophoresis, and immunoblot analyses were performed as previously described (9). Twenty micrograms of protein samples were applied to gels. The primary antibodies used in this study are shown in Table SI. Cell cycle assay was performed using a Cycletest Plus DNA Reagent Kit (BD Biosciences) as previously described (16).

Lentivirus production and transduction. Human *BCL2* cDNA was isolated from the pSVBT plasmid (a kind gift from Dr Tsujimoto) (17) by *Xho*I digestion and was cloned into pENTR1A (Invitrogen; Thermo Fisher Scientific, Inc.) at the *Sal*I-*Xho*I sites. Then, *BCL2* cDNA was subcloned into a lentivirus expression plasmid (pLenti6.3/V5-DEST, Invitrogen) with LR Clonase II (Invitrogen; Thermo Fisher Scientific, Inc.), and the resultant lentivirus plasmids were designated as *BCL2*/pLenti6.3. Lentiviruses were produced by the transfection of 293FT cells (Invitrogen; Thermo Fisher Scientific, Inc.) with *BCL2*/pLenti6.3 or EGFP/pLenti6.3 along with pLP1, pLP2, and pLP/VSVG (Invitrogen; Thermo Fisher Scientific, Inc.) mixtures using the Lipofectamine 2000 (Invitrogen) reagent according to the manufacturer's instructions. Cells were infected with lentivirus at a multiplicity of infection of five in the presence of 10 μg/ml of polybrene (Sigma-Aldrich; Merck KGaA) overnight and replaced with fresh media. After 48 h, the infected cells were selected using 10 μg/ml of blasticidin (Invitrogen; Thermo Fisher Scientific, Inc.).

Statistical analysis. Each experiment was performed in triplicate, and all data were shown as mean ± standard deviation. The Shapiro-Wilk test was used to evaluate whether data were normal distribution or not. The significance among three different groups was evaluated by one-way ANOVA. Then, for post hoc pairwise multiple comparisons, Tukey's test was used if Levene's test showed homogeneity of variance, and Games-Howell's test was used if not. P-value of <0.05 was considered a statistically significant difference. All statistical analyses were performed using the SPSS version 27.0 (SPSS, Inc.).

Results

Antitumor activity. We examined whether chiMDM4 could enhance the antitumor effects of chiMDM2 and trametinib

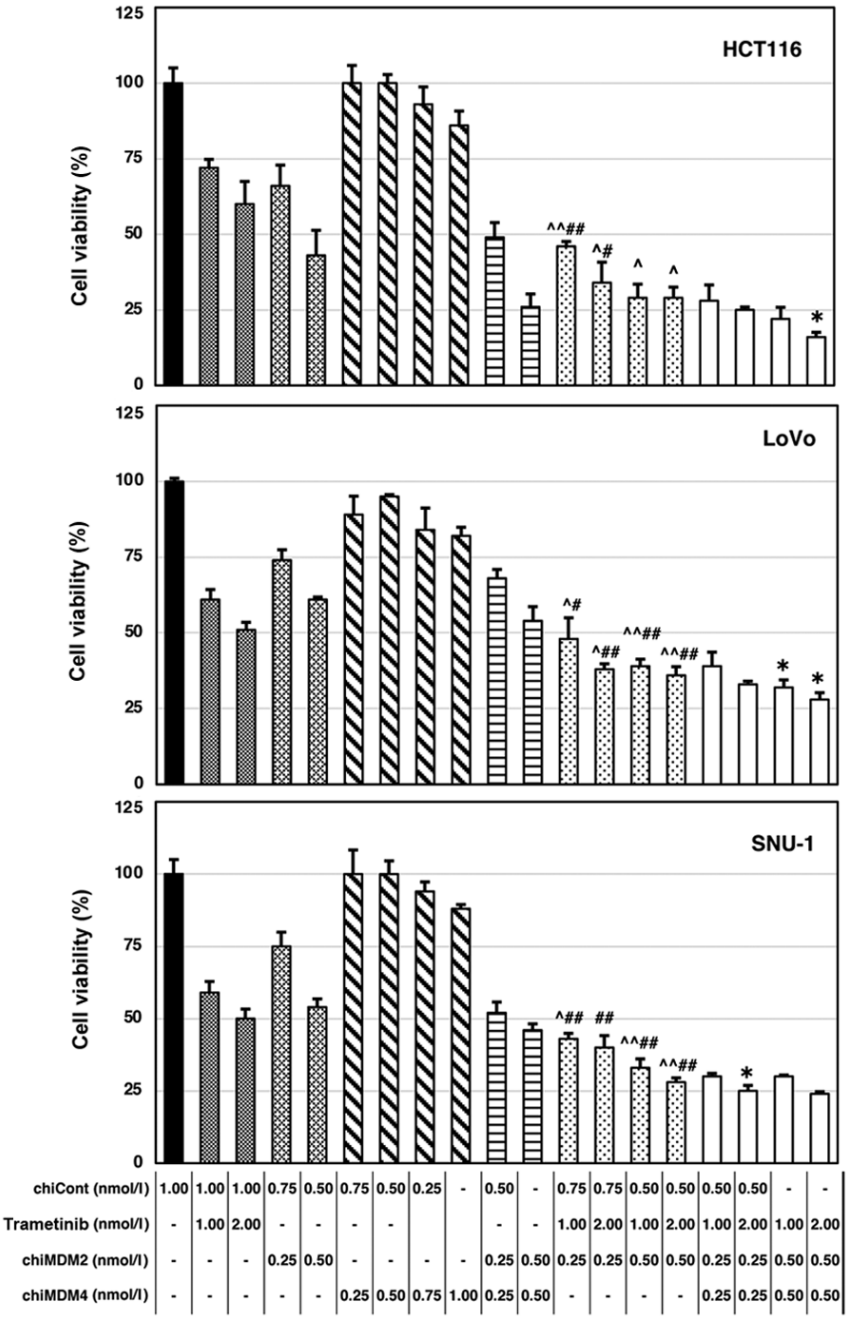

Figure 1. ChiMDM4/chiMDM2 and trametinib inhibited the growth of colon and gastric cancer cells. Cells were transfected with either chiCont, chiMDM2, chiMDM4 or an equimolar mixture of chiMDM4 and chiMDM2. Samples were then exposed to trametinib at the indicated concentrations and analyzed for cell viability. The viability of cancer cells transfected with the agents relative to those transfected with chiCont are presented (mean ± SD; n=3). Differences between multiple groups were evaluated using one-way ANOVA followed by Tukey's test. $^{\wedge}$P<0.05 and $^{\wedge\wedge}$P<0.01 vs. corresponding concentrations of the trametinib group. $^{\#}$P<0.05 and $^{\#\#}$P<0.01 vs. corresponding concentrations of the chiMDM2 group. *P<0.05 vs. corresponding concentrations of the chiMDM2+trametinib group. chiMDM, DNA-chimera small interfering RNA against MDM; Cont, control.

in colon (HCT116 and LoVo) and gastric (SNU-1) cancer cells harboring wt *TP53* and mt *KRAS* (wt/G13D). As shown in Fig. 1, trametinib alone and chiMDM2 alone decreased cell viability in a dose-dependent manner. Further, the combination of chiMDM2 and trametinib induced synergistic antitumor effects. The CIs of chiMDM4, chiMDM2, and trametinib were calculated and summarized (Table I). The addition of chiMDM4 augmented the antitumor effects of the combination of chiMDM2 and trametinib, which suggested that the simultaneous inhibition of MDM2 and MDM4 might have an advantage over the inhibition of MDM2 alone.

Similarly, we examined the cell viability after the treatment of cell lines with chiMDM4, nutlin-3, and trametinib (Fig. 2). The CI values of chiMDM4, nutlin-3, and trametinib are listed in Table II. The addition of chiMDM4 synergistically enhanced nutlin-3 and trametinib mediated growth suppression in the tumor cell lines.

Cell cycle distribution and apoptosis. To explore the mechanism by which trametinib treatment and dual inhibition of MDM4/MDM2 exerted an enhanced antitumor activity, their effects on cell cycle distribution and apoptosis were

Table I. Combination index of chiMDM2, trametinib and chiMDM4 in colon and gastric cancer cells.

A, HCT116 cell line

chiMDM2 (nmol/l)	Trametinib (nmol/l)	chiMDM4 (nmol/l)	Effect	Combination index
0.25	1.00	-	0.61	0.58
0.25	2.00	-	0.66	0.60
0.50	1.00	-	0.71	0.72
0.50	2.00	-	0.70	0.81
0.25	1.00	0.25	0.72	0.54
0.50	2.00	0.50	0.84	0.40

B, LoVo cell line

chiMDM2 (nmol/l)	Trametinib (nmol/l)	chiMDM4 (nmol/l)	Effect	Combination index
0.25	1.00	-	0.52	0.68
0.25	2.00	-	0.62	0.57
0.50	1.00	-	0.61	0.58
0.50	2.00	-	0.64	0.66
0.25	1.00	0.25	0.61	0.70
0.50	2.00	0.50	0.72	0.76

C, SNU-1 cell line

chiMDM2 (nmol/l)	Trametinib (nmol/l)	chiMDM4 (nmol/l)	Effect	Combination index
0.25	1.00	-	0.57	0.65
0.25	2.00	-	0.60	0.78
0.50	1.00	-	0.67	0.65
0.50	2.00	-	0.72	0.61
0.25	1.00	0.25	0.70	0.63
0.50	2.00	0.50	0.76	0.96

A combination index of <0.9 was defined as a synergistic effect. A combination index ≥0.9 and <1.1 was defined as an additive effect. A scombination index of ≥1.1 was defined as an antagonistic effect. chiMDM, DNA-chimera siRNA against MDM.

analyzed using flow cytometry (Fig. S2). As shown in Fig. 3, trametinib alone and chiMDM4/chiMDM2 alone increased the cell fractions in the G1 phase, whereas it reduced those in the S phases in all cell lines in a similar manner, which indicated an induced G1 arrest. Simultaneous exposure to trametinib and chiMDM4/chiMDM2 induced a profound G1 arrest. Trametinib alone did not or only slightly increased the sub-G1 population, which is representative of cells undergoing apoptotic cell death, whereas chiMDM4/chiMDM2 increased the sub-G1 population moderately in HCT116 and SNU-1 cells and slightly in LoVo cells. The combination of trametinib and chiMDM4/chiMDM2 further increased the sub-G1 population in all three cell lines. These results suggested that trametinib enhanced chiMDM4/chiMDM2-induced G1 arrest and apoptosis.

Alterations of cell cycle- and apoptosis-regulating proteins. The combination of trametinib and chiMDM4/chiMDM2 treatment induced the synergistic antitumor activity by enhancing G1 arrest and apoptosis in all cells with mt *KRAS*. To explore the mechanisms, proteins regulating cell cycle and apoptosis were examined in HCT116 cells using immunoblot analysis. Results were summarized using a heatmap (Fig. 4). If the upregulation or downregulation of the proteins by the combination of trametinib and chiMDM4/chiMDM2 was two-fold or more than the control and each agent alone, then it was considered as an important synergistic antitumor effect of the combination treatment. The proteins such as p53, p15, p27, and p53-activated proteins [p21, Fas, p53 upregulated modulator of apoptosis (PUMA), and 14-3-3 σ] were upregulated. On the other hand, the downregulated proteins included MDM2, p-ERK2, MYC, E2F1, and E2F1-activated proteins (cyclin A, cyclin B1, DNA polymerase δ, TYMS, CDC2, and CDC25A).

Effects on p-ERK2, p53, p21, RB, Fas and PUMA. We also analyzed the expression of those proteins in LoVo and SNU-1 cell lines that were greatly upregulated or downregulated in HCT116 cells (Fig. 5). Fold change values of the proteins

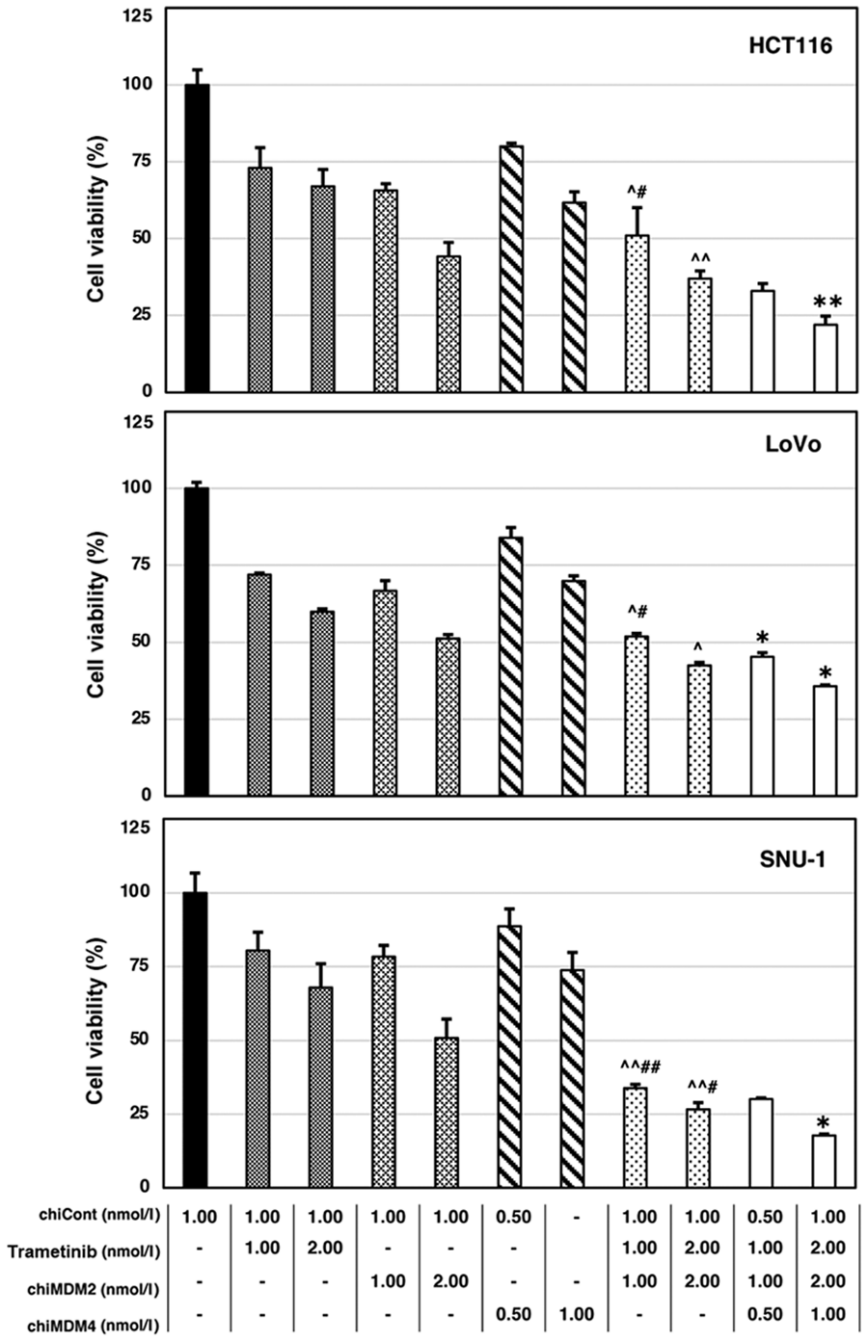

Figure 2. ChiMDM4, nutlin-3 and trametinib inhibited the growth of colon and gastric cancer cells. Cells were transfected with chiCont or chiMDM4, after which they were exposed to nutlin-3 and trametinib at the indicated concentrations and analyzed for cell viability. The viability of cancer cells transfected with the agents relative to those transfected with chiCont are presented (mean ± SD; n=3). Differences between multiple groups were evaluated using one-way ANOVA followed by Tukey's test. $^{\wedge}$P<0.05 and $^{\wedge\wedge}$P<0.01 vs. corresponding concentrations of the trametinib group; $^{\#}$P<0.05 and $^{\#\#}$P<0.01 vs. corresponding concentrations of the nutlin-3 group; *P<0.05 and **P<0.01 vs. corresponding concentrations of the nutlin-3+trametinib group. chiMDM, DNA-chimera small interfering RNA against MDM; Cont, control.

in all three cell lines are summarized in Table III. Notably, p-ERK2, which functions as a positive regulator of retinoblastoma (RB) phosphorylation and an inhibitor of cleavage of both caspase-8 and caspase-9, was suppressed by the combination of trametinib and chiMDM4/chiMDM2 treatment in all three cell lines (4.0-5.3-fold) compared to controls. With respect to the changes in protein expressions related to G1 arrest, the combination treatment markedly reduced phosphorylated RB (a master regulator of E2F-mediated transcription), cyclin A (one of the most efficiently activated proteins by E2F1), and MYC (a direct target of ERK1/2) in all three cell lines. ChiMDM4/chiMDM2 induced p53 and p21 in all three cell lines (Table III). In SNU-1 cells, as was observed in HCT116 cell, chiMDM4/chiMDM2 induced p53 and p21, which was enhanced by addition of trametinib. In LoVo cells, chiMDM4/chiMDM2 similarly induced p53 and p21. However, trametinib did not enhanced chiMDM4/chiMDM2-mediated p53 accumulation, or even decreased p21 accumulation. With regard to the changes in protein expressions related to apoptosis, chiMDM4/chiMDM2 induced moderate to high

Table II. Combination index of nutlin-3, trametinib and chiMDM4 in colon and gastric cancer cells.

A, HCT116 cell line

Nutlin-3 (μmol/l)	Trametinib (nmol/l)	chiMDM4 (nmol/l)	Effect	Combination index
1.00	1.00	-	0.49	0.72
2.00	2.00	-	0.63	0.84
1.00	1.00	0.50	0.67	0.56
2.00	2.00	1.00	0.78	0.59

B, LoVo cell line

Nutlin-3 (μmol/l)	Trametinib (nmol/l)	chiMDM4 (nmol/l)	Effect	Combination index
1.00	1.00	-	0.48	0.84
2.00	2.00	-	0.58	1.08
1.00	1.00	0.50	0.55	0.82
2.00	2.00	1.00	0.64	0.89

C, SNU-1 cell line

Nutlin-3 (μmol/l)	Trametinib (nmol/l)	chiMDM4 (nmol/l)	Effect	Combination index
1.00	1.00	-	0.66	0.45
2.00	2.00	-	0.73	0.72
1.00	1.00	0.50	0.70	0.85
2.00	2.00	1.00	0.83	0.53

A combination index of <0.9 was defined as a synergistic effect. A combination index ≥0.9 and <1.1 was defined as an additive effect. A combination index of ≥1.1 was defined as an antagonistic effect. chiMDM, DNA-chimera siRNA against MDM.

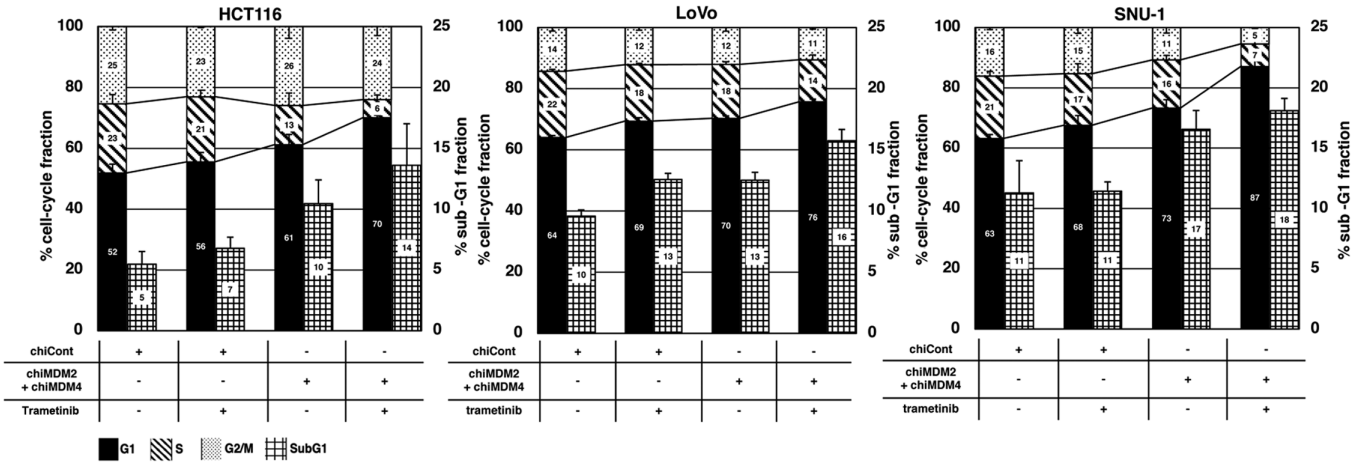

Figure 3. ChiMDM4/chiMDM2 and trametinib induced cell cycle arrest and apoptosis in colon and gastric cancer cells. Cells transfected with chiCont (1.0 nmol/l) or chiMDM4/chiMDM2 (0.5 nmol/l each) for 24 h were exposed to trametinib (2.0 nmol/l) for 24 h and analyzed for cell cycle distribution and apoptosis via flow cytometry. The bar height represents the fractions of each cell cycle phase and the sub-G1 phase. Data are presented as the means ± SD of triplicate experiments. chiMDM, DNA-chimera small interfering RNA against MDM; Cont, control.

levels of Fas in HCT116 and SNU-1 cells, and a low level of Fas in LoVo cells (Table III). The addition of trametinib increased Fas levels in HCT116, LoVo, and SNU-1 cells and markedly increased cleaved caspase-8 in HCT116 cells, and slightly increased it in LoVo cells; however, no increase of cleaved caspase-8 was detected in SNU-1 cells until twice the amount of protein samples was used in immunoblotting. Even so, trametinib slightly increased cleaved caspase-8 in chiMDM4/chiMDM2-treated SNU-1 cells (Fig. S3). ChiMDM4/chiMDM2 induced PUMA expression in HCT116

		Trametinib	chiMDM2 +chiMDM4	Combination
	MDM2	0.24	-1.74	-2.47
	MDM4	0.04	-0.60	-0.56
	p53	0.42	2.60	3.03
	phospho-ERK2	-1.89	-1.01	-2.84
	MYC	-0.64	-0.94	-1.80
G1-S progression	p21CIP1	1.03	3.96	4.04
	p15INK4B	0.20	1.48	1.64
	p27KIP1	-1.06	0.87	1.04
	CDK2	0.14	-0.56	-0.79
	CDK4	0.11	0.63	0.34
	cyclin D1	-0.22	2.36	1.66
	cyclin D3	0.18	0.80	0.21
	cyclin E2	0.08	0.18	0.10
	CDC25A	1.02	-0.76	-1.09
S phase	cyclin A	-0.60	-5.06	-6.64
	DNA polymerase δ	-0.07	-2.18	-2.74
	E2F1	0.00	-1.74	-2.18
	TYMS	-0.29	-1.51	-1.94
	RRM1	-0.01	-0.74	-0.95
	PCNA	0.04	-0.32	-0.42
	DNA polymerase α	0.42	0.56	0.61
G2-M phase	cyclin B1	-1.00	-4.64	-6.64
	CDC2	-0.30	-1.06	-1.22
	14-3-3 σ	0.24	1.10	1.29
Apoptosis	Fas	1.54	4.76	5.34
	DR4	-0.36	-0.62	-1.32
	DR5	ND	ND	ND
	BCL2	-0.58	-0.60	-0.58
	BAX	0.70	1.32	0.91
	PUMA	1.38	0.93	2.32
	APAF-1	0.15	0.00	0.15

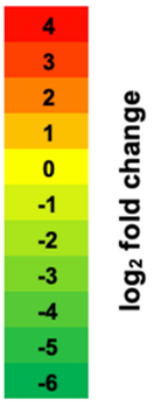

Figure 4. ChiMDM4/chiMDM2 and trametinib regulated the levels of cell cycle proteins involved in cell cycle progression and apoptosis induction in the HCT116 cell line. Cells were transfected with chiCont (1.0 nmol/l) or chiMDM4/chiMDM2 (0.5 nmol/l each) overnight, followed by exposure to trametinib (2.0 nmol/l) for 24 h, and then analyzed for protein expression by immunoblotting. β-actin was set as the internal control. Experiments were repeated three times and representative results are presented. The heatmap displays $\log_2$ fold changes of protein expression levels. Positive and negative values in the heatmap indicate fold-increase and fold-decrease relative to the control (chiCont-treated) cells. The red, yellow and green colors represent increased, unchanged, and decreased expressions relative to chiCont, respectively. chiMDM, DNA-chimera small interfering RNA against MDM; Cont, control; ND, not detected.

and LoVo cells, but not in SNU-1 cells. Trametinib further enhanced the expression of PUMA that was induced by chiMDM4/chiMDM2 in HCT116 and LoVo cells (Table III). This combination treatment caused caspase-9 cleavage in HCT116 and LoVo cells, but not in SNU-1 cells.

BCL2 induction in HCT116 and LoVo cells. Bcl2 is an antiapoptotic protein of Bcl2 family, regulating the mitochondria-mediated apoptosis in cells. Overexpression of Bcl2 antagonizes proapoptotic Bcl2 family members, such as PUMA, and represses caspase-9 activation by reducing the translocation of proapoptotic Bax and cytochrome C release, then inhibits the mitochondria-mediated apoptosis (18,19). To investigate whether activation of caspase-8 and caspase-9 was involved in the apoptosis caused by combination treatment, the effect of Bcl2 expression on apoptosis was analyzed in HCT116 and LoVo cells. *BCL2* and a control *EGFP* were stably transduced in HCT116 and LoVo cells using lentiviruses (Fig. 6A). As shown in Figs. 6B and S4, the combined treatment using chiMDM4/chiMDM2 and trametinib

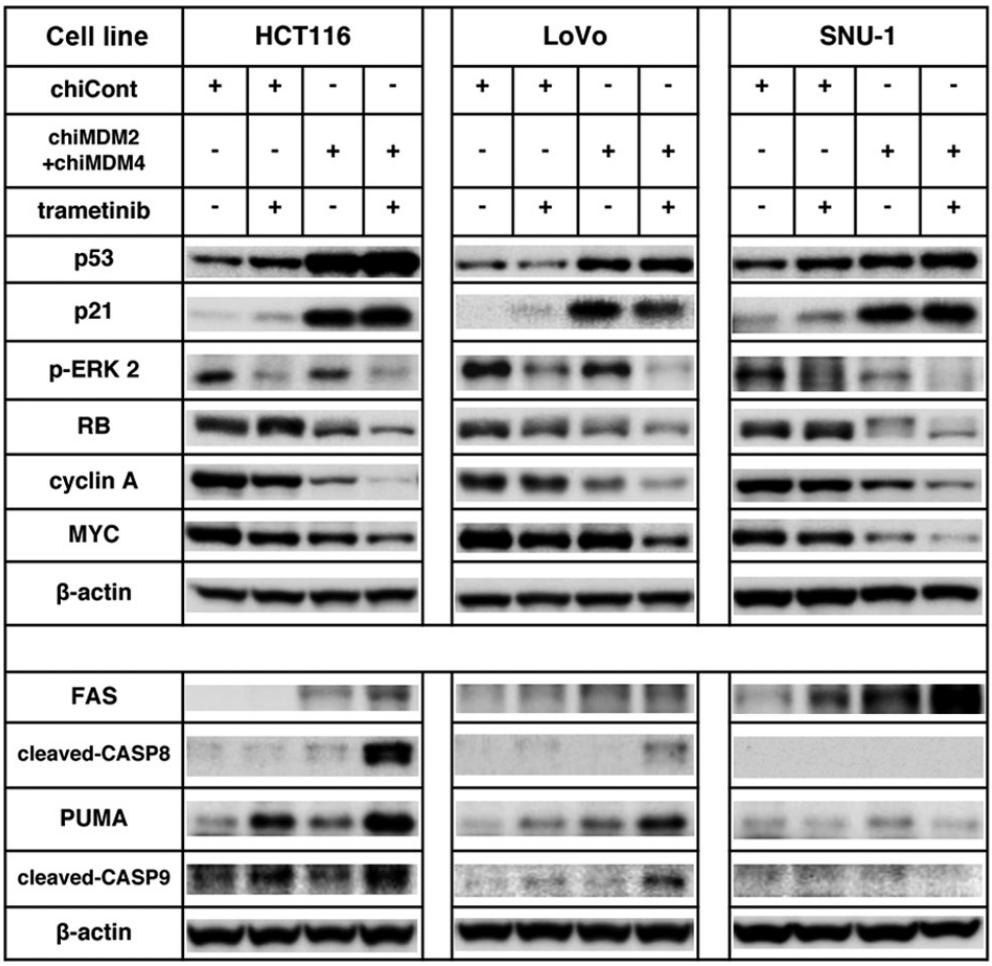

Figure 5. ChiMDM4/chiMDM2 and trametinib modulated protein levels of cell cycle progression and apoptosis regulation in colon and gastric cancer cells. For immunoblotting, 20 μg proteins were loaded per lane. Effects of chiMDM4/chiMDM2 and trametinib on p-ERK2, RB, MYC, cyclin A, PUMA and Fas levels were analyzed using immunoblotting in colon (HCT116 and LoVo) and gastric (SNU-1) cancer cells. Cells transfected with chiCont (1.0 nmol/l) or chiMDM4/chiMDM2 (0.5 nmol/l each) and trametinib (2.0 nmol/l) were analyzed via immunoblotting. β-actin was set as the internal control. chiMDM, DNA-chimera small interfering RNA against MDM; Cont, control; p, phosphorylated; ERK2, ERK, extracellular signal-regulated kinase 2; RB, retinoblastoma; PUMA, p53 upregulated modulator of apoptosis.

increased the sub-G1 population from 5 to 14% in the control HCT116 cells, whereas this combination increased the sub-G1 fraction from 3 to 7% in *BCL2*-transduced HCT116 cells. This suggests that Bcl2 overexpression partially blocks apoptosis induction in HCT116 cells via the combination treatment strategy. The combined treatment increased the sub-G1 fraction from 5 to 10% in the control LoVo cells and from 4 to 6% in *BCL2*-transduced LoVo cells, suggesting that Bcl2 overexpression strongly blocked apoptosis in LoVo cells via the combination treatment strategy.

Discussion

In this study, we confirmed the synergistic antitumor effect of MEK and MDM2 inhibition in colon and gastric cancer cells using the combination of trametinib and nutlin-3 and that of trametinib and chiMDM2 as a previous study (14). More importantly, we also showed that this synergistic antitumor effect was augmented by MDM4 knockdown. In our previous study, chiMDM4 strongly enhanced p53 activation mediated by nutlin-3 and chiMDM2 (9,10). Therefore, concurrent inhibition of MDM4 may greatly benefit this combination therapy in cancer cells with wt *TP53* harboring mt *KRAS*.

We demonstrated that enhanced induction of G1 arrest and apoptosis was the mechanism by which chiMDM4/chiMDM2 and trametinib exerted the synergistic antitumor effects in wt *TP53* colon and gastric cancer cells with *KRAS* mutations. This is schematized in Fig. 7. The extensive analysis of protein expressions in HCT116 cells revealed that chiMDM4/chiMDM2 intensely accumulated p53 and p21, which were associated with the downregulation of E2F1-activated proteins (cyclin A, cyclin B1, DNA polymerase δ, E2F1, and TYMS) and upregulation of pro-apoptotic proteins (Fas and PUMA). Although trametinib alone induced only subtle changes in these protein levels other than p-ERK2, cyclin B1, and p21, it enhanced the alterations caused by chiMDM4/chiMDM2. These synergistic antitumor effects of chiMDM4/chiMDM2 and trametinib might involve the interaction between ERK1/2 and MDM2. Because activated ERK1/2 upregulates MDM2 at the transcriptional and post-translational levels (12,13), trametinib and chiMDM2 may cooperatively suppress MDM2 expression at various levels of transcription, post-transcription, and post-translation, leading to further accumulation of p53.

Table III. Changes in phosphorylated-ERK, cyclin A, Fas and PUMA levels induced by chiMDM4/chiMDM2 and trametinib in colon and gastric cancer cells.

A, HCT116 cell line

	Fold change relative to control		
Up/downregulated cell cycle apoptosis regulating protein	Trametinib	chiMDM2 + chiMDM4	Combination
Upregulated			
p53	1.6	7.7	11.3
p21CIP1	2.0	19.5	21.8
Fas	2.9	27.1	40.4
PUMA	2.6	1.9	5.0
Downregulated			
Phospho-ERK2	2.2	1.0	5.0
MYC	1.6	2.9	3.5
Cyclin A	1.4	4.6	16.7

B, LoVo cell line

	Fold change relative to control		
Up/downregulated cell cycle apoptosis regulating protein	Trametinib	chiMDM2 + chiMDM4	Combination
Upregulated			
p53	1.3	3.1	3.1
p21CIP1	3.0	20.4	13.4
Fas	1.1	1.2	1.3
PUMA	1.9	2.1	4.2
Downregulated			
Phospho-ERK2	2.1	1.4	5.3
MYC	1.5	1.5	4.4
Cyclin A	1.3	2.3	4.2

C, SNU-1 cell line

	Fold change relative to control		
Up/downregulated cell cycle apoptosis regulating protein	Trametinib	chiMDM2 + chiMDM4	Combination
Upregulated			
p53	1.4	2.0	2.9
p21CIP1	3.7	14.2	18.0
Fas	2.1	3.3	5.1
PUMA	1.1	2.2	1.7
Downregulated			
Phospho-ERK2	1.8	1.1	4.0
MYC	1.5	3.3	6.7
Cyclin A	1.4	2.3	5.6

Alterations to immunoblot band intensities relative to control DNA-chimera siRNA (chiCont) are presented according to fold change. ERK2, extracellular signal-regulated kinase 2; PUMA, p53 upregulated modulator of apoptosis; CIP1, CDK-interacting protein 1; chiMDM, DNA-chimera siRNA against MDM; siRNA, small interfering RNA.

The combination of chiMDM4/chiMDM2 and trametinib altered the expression levels of phosphorylated RB and E2F-activated molecules more intensely than the p53 and CDK inhibitor (p21, p15 and p27) levels in HCT116

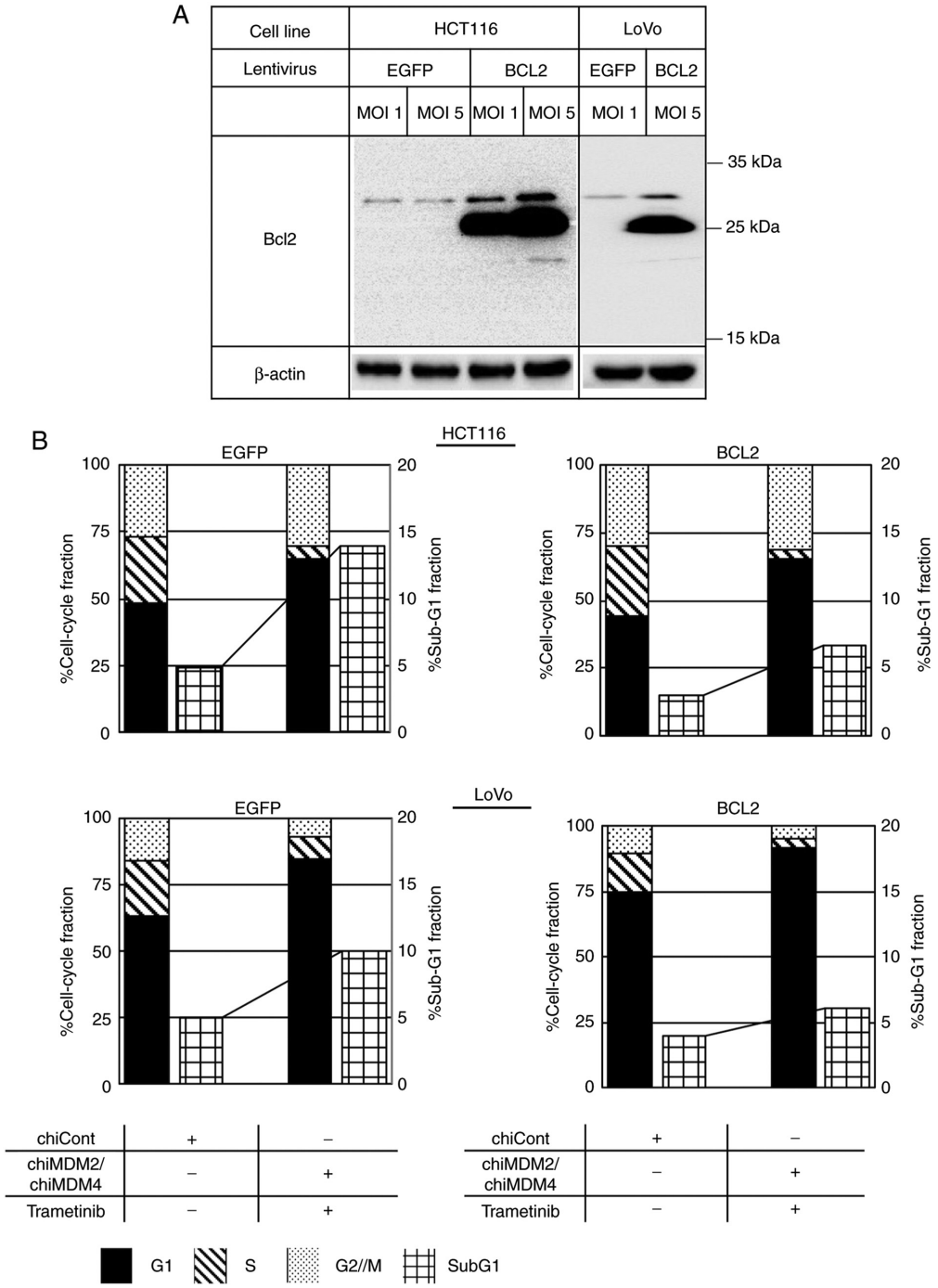

Figure 6. *BCL2* induction suppressed chiMDM4/chiMDM2- and trametinib-mediated apoptosis to a greater extent in LoVo cells compared with HCT116 cells. (A) *BCL2* was stably transduced in HCT116 and LoVo cells using lentiviruses. Bcl2 expressions were examined by immunoblotting. Bcl2 (28 kDa) was detected in *EGFP*- and BCL2-transduced HCT116 cells and LoVo cells whereas an intense accumulation of Bcl2 (26 kDa) was seen in *BCL2*-transduced HCT116 and Lovo cells. This 26 kDa Bcl2 in *BCL2*-transduced cells possesses an anti-apoptotic activity. (B) *EGFP*-transduced HCT116 cells and LoVo cells were transfected with chiCont (1.0 nmol/l) or chiMDM4/chiMDM2 (0.5 nmol/l each) for 24 h, followed by exposure to trametinib (2.0 nmol/l) for 24 h, and the cell cycle distribution and apoptosis were analyzed by flow cytometry. The bar height represents the fractions of each cell cycle phase and the sub-G1 phase. chiMDM, DNA-chimera small interfering RNA against MDM; Cont, control; EGFP, enhanced green fluorescent protein; kDa, kilodalton.

cells (Figs. 4, 5 and Table III). Trametinib enhanced neither chiMDM4/chiMDM2-induced accumulation of p53 nor p21 in LoVo cells. These results suggest that activation of p53-p21-RB pathway may not be a sole mechanism of synergistic growth suppression; it might be regulated by some other pathways. ERK1/2 directly participates in the regulation of RB phosphorylation (20). Hypo-phosphorylated RB binds to lamin A, forms a complex with E2F and E2F-regulated promoters, and inhibits E2F-transcriptional activity. Phosphorylated ERK1/2 enters the nucleus and competes with RB at the same binding site of lamin A and thereby releases RB. Free RB is rapidly phosphorylated and consequently promotes cell cycle progression by E2F1-mediated gene expression (20). Suppression of ERK1/2 phosphorylation by trametinib might coordinately inhibit RB phosphorylation with p53 activation induced by chiMDM4/chiMDM2.

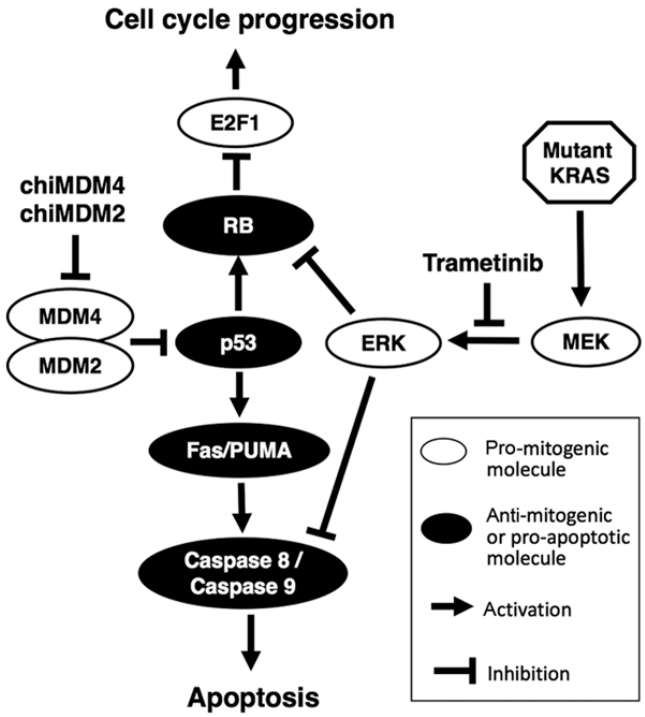

Figure 7. Molecular mechanisms involved in chiMDM4, chiMDM2 and trametinib-mediated cell cycle arrest and apoptosis. ChiMDM4 and chiMDM2 reactivates p53, which decreases phosphorylated RB levels. The MEK inhibitor, trametinib, inhibits the downstream signaling pathway of mutant KRAS. RB phosphorylation is also reduced by ERK inhibition. As a result, E2F1 is inhibited by both pathways. Simultaneously, activated p53 induces pro-apoptotic proteins, and inhibition of ERK by trametinib promotes the same apoptosis pathway. chiMDM, DNA-chimera small interfering RNA against MDM; RB, retinoblastoma; MEK, mitogen-activated protein kinase kinase; ERK, extracellular signal-regulated kinase; MDM2/4, murine double minute homolog 2/4.

Trametinib enhanced chiMDM4/chiMDM2-induced apoptosis in all the cell lines used in this study. It has been reported that MDM2 and MEK inhibition increased the levels of Bcl2-like protein 11 and PUMA and attributed the induction of apoptosis as a reason for their accumulation in some cell lines (14). We found that our combination treatment similarly stimulated the intrinsic pathway involving PUMA-caspase-9 in HCT116 and LoVo cells and also the extrinsic apoptotic pathway involving Fas-caspase-8 in HCT116 cells and to a lesser extent in LoVo and SNU-1 cells. The weaker cleaved caspase-8 induction by chiMDM4/chiMDM2 and trametinib, which is a little inconsistent with certainly induced apoptosis in cell cycle assay in SNU-1 cells, suggests that chiMDM4/chiMDM2 and trametinib may induce caspase dependent as well as caspase independent apoptosis in SNU-1 cells (21-23). *BCL2* transduction inhibited apoptosis more efficiently in LoVo cells than HCT116 cells, suggesting that PUMA-caspase-9 pathway might be the major signaling in the combination-induced apoptosis in LoVo cells whereas the combination-induced apoptosis in HCT116 cells might involve both Fas-caspase-8 and PUMA-caspase-9 pathways. These some differences observed in the caspase-8 and caspase-9 activation among three cell lines could be attributed to the different inducibility or expressed levels of pro- and anti-apoptotic proteins regulating apoptosis. Because ERK1/2 inhibits pro-caspase-8 and pro-caspase-9 cleavage by phosphorylating residues at the S387 (24) and T125 (25) sites, respectively, trametinib can enhance apoptosis via both caspase-8- and caspase-9-mediated routes.

This study has two methodological limitations. First, all cell lines used in our study harbored mt *KRAS*. Hence, it may be difficult to reach a definitive conclusion as to whether the *KRAS* mutation status affects the synergistic effect of the chiMDM4/chiMDM2 and trametinib combination treatment. Second, the three cancer cell lines with mt *KRAS* harbored *PIK3CA* or *PIK3CB* mutations. *PIK3CA* mutation (H1047R) of HCT116 cells and *PIK3CB* mutation (E1051K) of LoVo cells are pathogenic. We did not examine the interaction between the PI3K-PTEN-Akt and p53 pathways as this might also affect the synergistic effects observed in this study. There remains another issue about toxicities of this combination treatment. To resolve these issues, further studies are warranted.

In conclusion, enhanced p53 activation by MDM4/MDM2 knockdown and trametinib treatment exerted the synergistic antitumor activity through G1 arrest and apoptosis in wt *TP53* gastrointestinal cancers with aberrant KRAS signaling. This simultaneous MDM2, MDM4, and MEK-ERK inhibition may be a promising therapy for gastrointestinal cancers.

Acknowledgements

Not applicable.

Funding

This work was supported by the Japanese Society for the Promotion of Science (JSPS KAKENHI; grant no. JP18K07288).

Availability of data and material

The datasets used and/or analyzed during the current study are available from the corresponding author on reasonable request.

Authors' contributions

XW, YY, YN, TM, KY, and IH conceived and designed the study. XW, MI, XZ, MS, AS, MH, SE and KY performed the experiments. YY, KY, and IH confirm the authenticity of all the raw data. XW and YY performed the statistical analyses. XW, YY, and IH wrote the manuscript. All authors read and approved the final manuscript.

Ethics approval and consent to participate

Not applicable.

Patient consent for publication

Not applicable.

Competing interests

The authors declare that they have no competing interests.

References

1. Sionov RV and Haupt Y: The cellular response to p53: The decision between life and death. Oncogene 18: 6145-6157, 1999.
2. Vousden KH and Lu X: Live or let die: The cell's response to p53. Nat Rev Cancer 2: 594-604, 2002.
3. Levine AJ: The tumor suppressor genes. Annu Rev Biochem 62: 623-651, 1993.
4. Moll UM and Petrenko O: The MDM2-p53 interaction. Mol Cancer Res 1: 1001-1008, 2003.
5. Linares LK, Hengstermann A, Ciechanover A, Müller S and Scheffner M: HdmX stimulates Hdm2-mediated ubiquitination and degradation of p53. Proc Natl Acad Sci USA 100: 12009-12014, 2003.
6. Shvarts A, Steegenga WT, Riteco N, van Laar T, Dekker P, Bazuine M, van Ham RC, van der Houven van Oordt W, Hateboer G, van der Eb AJ and Jochemsen AG: MDMX: A novel p53-binding protein with some functional properties of MDM2. EMBO J 15: 5349-5357, 1996.
7. Wu X, Bayle JH, Olson D and Levine AJ: The p53-mdm-2 autoregulatory feedback loop. Genes Dev 7: 1126-1132, 1993.
8. Mahmoodi Chalbatani G, Dana H, Gharagouzloo E, Grijalvo S, Eritja R, Logsdon CD, Memari F, Miri SR, Rad MR and Marmari V: Small interfering RNAs (siRNAs) in cancer therapy: A nano-based approach. Int J Nanomedicine 14: 3111-3128, 2019.
9. Imanishi M, Yamamoto Y, Wang X, Sugaya A, Hirose M, Endo S, Natori Y, Yamato K and Hyodo I: Augmented antitumor activity of 5-fluorouracil by double knockdown of MDM4 and MDM2 in colon and gastric cancer cells. Cancer Sci 110: 639-649, 2019.
10. Hirose M, Yamato K, Endo S, Saito R, Ueno T, Hirai S, Suzuki H, Abei M, Natori Y and Hyodo I: MDM4 expression as an indicator of TP53 reactivation by combined targeting of MDM2 and MDM4 in cancer cells without TP53 mutation. Oncoscience 1: 830-843, 2014.
11. Endo S, Yamato K, Hirai S, Moriwaki T, Fukuda K, Suzuki H, Abei M, Nakagawa I and Hyodo I: Potent in vitro and in vivo antitumor effects of MDM2 inhibitor nutlin-3 in gastric cancer cells. Cancer Sci 102: 605-613, 2011.
12. Malmlöf M, Roudier E, Högberg J and Stenius U: MEK-ERK-mediated phosphorylation of Mdm2 at Ser-166 in hepatocytes. Mdm2 is activated in response to inhibited Akt signaling. J Biol Chem 282: 2288-2296, 2007.
13. Ries S, Biederer C, Woods D, Shifman O, Shirasawa S, Sasazuki T, McMahon M, Oren M and McCormick F: Opposing effects of Ras on p53: Transcriptional activation of mdm2 and induction of p19ARF. Cell 103: 321-330, 2000.
14. Hata AN, Rowley S, Archibald HL, Gomez-Caraballo M, Siddiqui FM, Ji F, Jung J, Light M, Lee JS, Debussche L, *et al*: Synergistic activity and heterogeneous acquired resistance of combined MDM2 and MEK inhibition in KRAS mutant cancers. Oncogene 36: 6581-6591, 2017.
15. Chou TC and Talalay P: Quantitative analysis of dose-effect relationships: The combined effects of multiple drugs or enzyme inhibitors. Adv Enzyme Regul 22: 27-55, 1984.
16. Bronkhorst AJ, Wentzel JF, Aucamp J, van Dyk E, du Plessis L and Pretorius PJ: Characterization of the cell-free DNA released by cultured cancer cells. Biochim Biophys Acta 1863: 157-165, 2016.
17. Tsujimoto Y and Croce CM: Analysis of the structure, transcripts, and protein products of bcl-2, the gene involved in human follicular lymphoma. Proc Natl Acad Sci USA 83: 5214-5218, 1986.
18. Yang J, Liu X, Bhalla K, Kim CN, Ibrado AM, Cai J, Peng TI, Jones DP and Wang X: Prevention of apoptosis by Bcl-2: Release of cytochrome c from mitochondria blocked. Science 275: 1129-1132, 1997.
19. Reshi L, Wang HV, Hui CF, Su YC and Hong JR: Anti-apoptotic genes Bcl-2 and Bcl-xL overexpression can block iridovirus serine/threonine kinase-induced Bax/mitochondria-mediated cell death in GF-1 cells. Fish Shellfish Immunol 61: 120-129, 2017.
20. Rodríguez J, Calvo F, González JM, Casar B, Andrés V and Crespo P: ERK1/2 MAP kinases promote cell cycle entry by rapid, kinase-independent disruption of retinoblastoma-lamin A complexes. J Cell Biol 191: 967-979, 2010.
21. Bidère N and Senik A: Caspase-independent apoptotic pathways in T lymphocytes: A minireview. Apoptosis 6: 371-375, 2001.
22. Wu M, Xu LG, Li X, Zhai Z and Shu HB: AMID, an apoptosis-inducing factor-homologous mitochondrion-associated protein, induces caspase-independent apoptosis. J Biol Chem 277: 25617-25623, 2002.
23. Lee TJ, Kim EJ, Kim S, Jung EM, Park JW, Jeong SH, Park SE, Yoo YH and Kwon TK: Caspase-dependent and caspase-independent apoptosis induced by evodiamine in human leukemic U937 cells. Mol Cancer Ther 5: 2398-2407, 2006.
24. Mandal R, Raab M, Matthess Y, Becker S, Knecht R and Strebhardt K: pERK 1/2 inhibit caspase-8 induced apoptosis in cancer cells by phosphorylating it in a cell cycle specific manner. Mol Oncol 8: 232-249, 2014.
25. Allan LA, Morrice N, Brady S, Magee G, Pathak S and Clarke PR: Inhibition of caspase-9 through phosphorylation at Thr 125 by ERK MAPK. Nat Cell Biol 5: 647-654, 2003.